

Static and Dynamic Magnetic Properties of Spin-1/2 Inequilateral Diamond-Chain Compounds $A_3\text{Cu}_3\text{AlO}_2(\text{SO}_4)_4$ ($A=\text{K}, \text{Rb}, \text{and Cs}$)

Katsuhiro Morita,^{1,*} Masayoshi Fujihala,² Hiroko Koorikawa,² Takanori Sugimoto,¹ Shigetoshi Sota,³ Setsuo Mitsuda,² and Takami Tohyama¹

¹*Department of Applied Physics, Tokyo University of Science, Tokyo 125-8585, Japan*

²*Department of Physics, Tokyo University of Science, Shinjuku, Tokyo 162-8601, Japan*

³*RIKEN Advanced Institute for Computational Science (AICS), Kobe, Hyogo 650-0047, Japan*

(Dated: March 19, 2019)

Spin-1/2 compounds $A_3\text{Cu}_3\text{AlO}_2(\text{SO}_4)_4$ ($A=\text{K}, \text{Rb}, \text{and Cs}$) have one-dimensional (1D) inequilateral diamond chains. We analyze the temperature dependence of the magnetic susceptibility and determine the magnetic exchange interactions. In contrast to the azurite, a dimer is formed on one of the sides of the diamond. From numerical analyses of the proposed model, we find that the dimer together with a nearly isolated 1D Heisenberg chain characterizes magnetic properties including magnetization curve and magnetic excitations. This implies that a dimer-monomer composite chain without frustration is a good starting point for describing these compounds.

PACS numbers: 75.10.Jm, 75.10.Kt, 75.60.Ej

Highly frustrated quantum magnets provide various exotic ground states such as gapless spin-liquid and gapped singlet dimer phases [1–3]. In a magnetic field, the magnets exhibit magnetization plateaus because of the competition of frustration and quantum fluctuations. The typical constituent of frustrated magnets is a triangular unit of spin with antiferromagnetic (AFM) interaction for each bond. The spin-1/2 diamond chain, where the triangular unit is connected linearly, is thus regarded as a typical highly frustrated system in one dimension [4–6].

The azurite $\text{Cu}_3(\text{CO}_3)_2(\text{OH})_2$ has originally been suggested to be a spin-1/2 distorted diamond chain with AFM interactions for three bonds of a triangular unit [7]. A recent theoretical approach based on density functional theory together with numerical many-body calculations has proposed a microscopic model of the azurite with less frustrated interactions [8]: two of three Cu^{2+} spins are strongly coupled by AFM interaction J_2 (see Fig. 1(b)) to form a dimer singlet, while another spin consists of a monomer spin that is weakly connected to neighboring monomer spins by AFM interaction J_m . This model including the two energy scales of J_2 and J_m has nicely reproduced the double-peak structures observed in the magnetic susceptibility (a peak at 5 K and a broad peak at 23 K) [7] and the specific heat [7, 9]. In a magnetic field, the 1/3 magnetization plateau [7] is interpreted as a result of almost fully polarized monomer spins and bounded dimer spins [8]. The model predicts a gapless low-energy spin excitation originating from a spin liquid behavior due to an effective spin-1/2 Heisenberg chain [10]. However, three-dimensional magnetic interactions in the azurite cause the magnetic order below 1.85 K.

Recently, a new highly one-dimensional (1D) diamond chain compound $\text{K}_3\text{Cu}_3\text{AlO}_2(\text{SO}_4)_4$ has been reported [11]. In this compound, the magnetic suscep-

tibility exhibits a double-peak structure similar to the azurite, but the temperatures of the peaks (50 K and 200 K) are one-order higher than those in the azurite. In spite of such high characteristic temperatures, there is no magnetic order down to 0.5 K, indicating a possible spin-liquid ground state [11]. It is, thus, important to clarify common features characterizing the distorted diamond-chain compounds in both the azurite and the new compound.

In this Letter, we analyze the temperature dependence of the magnetic susceptibility in $\text{K}_3\text{Cu}_3\text{AlO}_2(\text{SO}_4)_4$ as well as newly synthesized compounds, where Rb and Cs are substituted for K, by using the exact diagonalization (ED) method. The estimated magnetic exchange interactions are found to form strong dimer bond and monomer-monomer chains. This is similar to the azurite, although the dimer-bond position as well as their energy scale is different. The frustration is less effective in $\text{K}_3\text{Cu}_3\text{AlO}_2(\text{SO}_4)_4$ than in the azurite and the spin-liquid behavior at low temperatures is attributed to an effective spin-1/2 Heisenberg chain. Therefore, it is reasonable to conclude that diamond chain compounds consisting of Cu^{2+} are less frustrated materials, and thus a good starting point of the compounds is a dimer-monomer composite structure. Based on the estimated exchange interactions in $\text{K}_3\text{Cu}_3\text{AlO}_2(\text{SO}_4)_4$, we predict the magnetization curve with the 1/3 plateau and inelastic neutron scattering spectrum by density matrix renormalization group (DMRG) calculations.

The crystal structure of $A_3\text{Cu}_3\text{AlO}_2(\text{SO}_4)_4$ ($A = \text{K}, \text{Rb}, \text{and Cs}$) is shown in Fig. 1(a). The diamond chains composed of Cu^{2+} ions are formed along the a axis. Since the diamonds are inequilateral, as be discussed below, exchange interactions for the nearest-neighbor bonds (J_1 to J_5 as shown in Fig. 1(b)) are not necessarily the same. In addition, we consider exchange interactions connecting neighboring triangular units, denoted by J_m , J_d , and J'_d

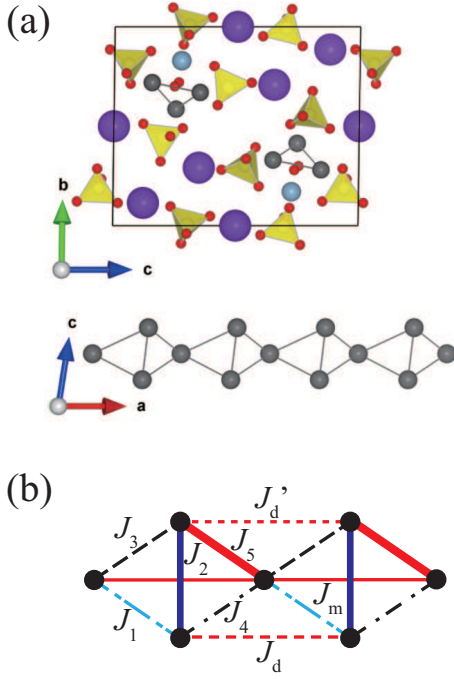


FIG. 1. (Color online) (a) Crystal structure of $A_3Cu_3AlO_2(SO_4)_4$ ($A = K, Rb$, and Cs). The gray, purple, light blue, and red circles denote Cu , A , Al , and O atoms, respectively. The tetrahedrons with the red dots at the corners denote (SO_4). The inequilateral diamond chains run along the a axis. (b) Effective spin model of $A_3Cu_3AlO_2(SO_4)_4$. The circles represent Cu^{2+} ions with spin $1/2$. The blue broken, dark blue solid, black broken, black dash-dot, red thick solid, red thin solid, red dashed, and red dotted lines denote the exchange interactions J_1 , J_2 , J_3 , J_4 , J_5 , J_m , J_d , and J_d' , respectively.

in Fig. 1(b). We note that only J_m is taken into account in the azurite. In the present compounds there are possible paths for the J_d and J_d' bonds through SO_4 units. Since the surrounding components of the three J_m , J_d , and J_d' bonds are similar to each other, we assume that $J_m = J_d = J_d'$.

The effective spin Hamiltonian for $A_3Cu_3AlO_2(SO_4)_4$ under the external magnetic field H is thus given by

$$\mathcal{H} = \sum_{\langle i,j \rangle} J_{ij} \mathbf{S}_i \cdot \mathbf{S}_j - g\mu_B H \sum_i S_i^z, \quad (1)$$

where \mathbf{S}_i is the spin- $1/2$ operator, J_{ij} is the exchange interactions corresponding to the bonds shown in Fig 1(b), μ_B is the Bohr magneton, and g is the gyromagnetic ratio.

Before fitting calculated magnetic susceptibilities to experimental ones, we need to roughly evaluate the value of exchange interactions. From the crystal structure analysis of $K_3Cu_3AlO_2(SO_4)_4$, the average $Cu-O-Cu$ angle is estimated to be $104.7^\circ, 95.2^\circ, 102.5^\circ, 105.8^\circ$, and 132.0° for the J_1 , J_2 , J_3 , J_4 , and J_5 bond, respectively [12]. Since the $Cu-O-Cu$ angle significantly influences on the

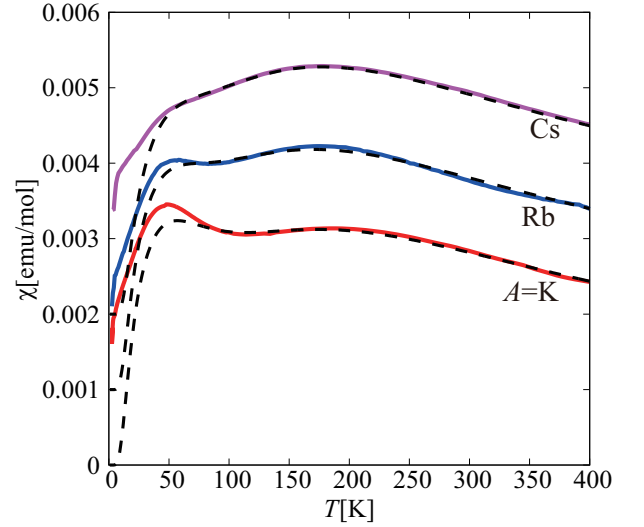


FIG. 2. (Color online) Temperature dependence of spin susceptibility in $A_3Cu_3AlO_2(SO_4)_4$ ($A = K, Rb$, and Cs). The solid lines show the experimental data. The dotted lines represent the fitted data obtained by the ED calculations for an 18-spin inequilateral diamond chain. The parameters are listed in Table I. The data are shifted upward by 0.001 emu/mol for $A = Rb$ and 0.002 emu/mol for $A = Cs$.

value of exchange interactions [13], the variation of the angles can give strongly bond-dependent exchange interactions. According to the angle-dependent exchange interaction of cuprates [13], J_5 with the largest angle is expected to be an AFM interaction with very roughly ~ 500 K, while J_2 with the smallest angle is to be ferromagnetic (FM) (~ -100 K). The value of exchange interactions for other bonds are expected to be in between J_2 and J_5 . For simplicity, we take $J_1 = J_3 = J_4$ because of similar $Cu-O-Cu$ angles. We emphasize that the side of the J_1 bond and the side of the J_5 bond, which are opposite sides of a diamond, are inequivalent. This means that the diamond is distorted making opposite sides inequivalent, i.e., an inequilateral diamond. We thus call $A_3Cu_3AlO_2(SO_4)_4$ the inequilateral diamond chain compound.

Taking into account this initial guess for the exchange interactions, we first investigate the temperature dependence of the spin susceptibility for $K_3Cu_3AlO_2(SO_4)_4$ by performing the ED calculations for an 18-site diamond periodic chain [six triangular units (the total number of site $N = 6 \times 3$)]. The calculated spin susceptibility χ is compared to the experimental data [11] obtained by subtracting the diamagnetic susceptibility χ_{dia} , the impurity-spin paramagnetic susceptibility χ_{imp} , and the Van Vleck paramagnetic susceptibility χ_{VV} [14] from the experimentally observed magnetic susceptibility. Figure 2 shows the experimental and fitted results of χ for $K_3Cu_3AlO_2(SO_4)_4$ (red solid line and black dashed line). The parameter values are listed in Table I. The fitted re-

TABLE I. The exchange interactions and the gyromagnetic ratio obtained by fitting calculated χ to experimental ones.

A	$J_1 = J_3 = J_4$	J_2	J_5	$J_m = J_d = J'_d$	g
K	-30	-300	510	75	2.14
Rb	-17	-252	462	84	2.12
Cs	-19	-238	456	95	2.17

sult deviates from the experimental data at $T < 70$ K, which is due to the finite size effect of the ED calculation as confirmed by system-size dependence (not shown here). However, the double-peak structure is clearly reproduced. We find that a broad peak at 200 K comes from large J_5 forming a dimer on the corresponding bond, while the low-temperature peak at 50 K is attributed to a 1D Heisenberg interaction with positive J_d , being similar to the case of the azurite. The other parameters only affect the heights of the two peaks.

The obtained value of J_5 is the largest and fifteen times larger than the maximum interaction in the azurite (~ 33 K). Similarly J_d ($= J'_d = J_m$) in $A = \text{K}$ is sixteen times larger than J_m in the azurite (~ 4.62 K). Another important difference appears on the J_2 bond: J_2 is FM in $\text{K}_3\text{Cu}_3\text{AlO}_2(\text{SO}_4)_4$, while the dimer is located on the bond in the azurite. It is also remarkable that there is only weak frustration in the diamond of $\text{K}_3\text{Cu}_3\text{AlO}_2(\text{SO}_4)_4$, since the magnitude of FM J_4 interaction inducing frustration in a triangle is very small as compared with two other interactions J_2 and J_5 .

To confirm the magnetic interactions on A -site substituted compounds, we synthesized single phase crystalline with $A = \text{Rb}$ and Cs by a solid-state reaction in which high-purity A_2SO_4 , CuO , CuSO_4 and $\text{AlK}(\text{SO}_4)_2$ powder were mixed with molar ratio of 1 : 2 : 1 : 1. The mixture was heated at 600°C for three days and then slowly cooled in air.

We fit calculated χ to the experimental ones for $A = \text{Rb}$ and Cs in Fig. 2. The two-peak structure is less pronounced but visible for $A = \text{Cs}$. From the estimated parameter values of the exchange interactions listed in Table I, we find that J_5 for $A = \text{Rb}$ and Cs is 10% smaller than that for $A = \text{K}$. Actually the broad peak position shifts to lower temperature by nearly the same amount. This change of J_5 is consistent with a reduction of the Cu-O-Cu bond angle from $A = \text{K}$ to $A = \text{Rb}$ and Cs [12]. In contrast, J_d ($= J'_d = J_m$) increases from $A = \text{K}$, Rb , to Cs , inducing a slight shift of the low-temperature peak to high temperature. Other parameters with FM interactions reduce their magnitude from $A = \text{K}$ to Rb and Cs . These material dependent change of the interactions indicate a small change of Cu-O-Cu bond angles between K and Rb (Cs). A detailed crystal structure analyses will be necessary to confirm this and remains as a future problem.

To confirm the validity of the estimated exchange

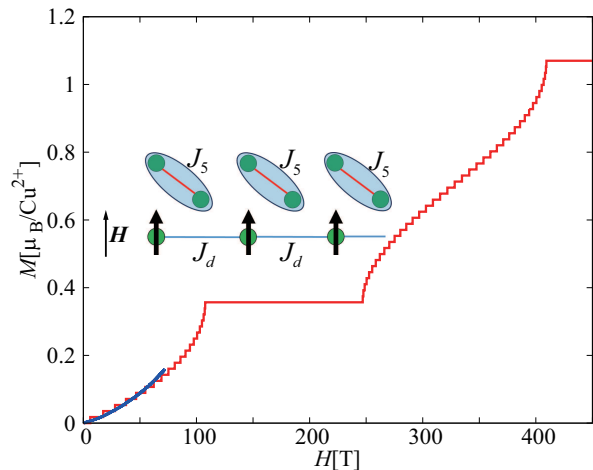


FIG. 3. (Color online) Magnetization curve for $\text{K}_3\text{Cu}_3\text{AlO}_2(\text{SO}_4)_4$. The red jagged solid line is calculated curve by DMRG at zero temperature for a 120-site periodic chain with the exchange interactions estimated from χ . The blue solid line represents the experimental result under the magnetic field up to 72 T at 4.2 K [11]. The inset is a schematic view of spin configuration at the $1/3$ plateau with the dimers formed by J_5 and the 1D chain with J_d whose spins are ferromagnetically aligned to the direction of the applied magnetic field H .

interactions, we calculate the magnetization curve for $\text{K}_3\text{Cu}_3\text{AlO}_2(\text{SO}_4)_4$ and compare it with available experimental data [11]. The magnetization curve is calculated by DMRG for a $N = 120 (= 40 \times 3)$ -site periodic chain at zero temperature. The number of states kept in the DMRG calculation is $m = 300$ and the resulting truncation error is less than 2×10^{-6} . Figure 3 shows the calculated magnetization curve as well as the experimental data for low magnetic field up to $H = 72$ T [11]. The agreement with the experimental data is quite well. The magnetization near zero field is proportional to H , which is characteristic behavior in the 1D Heisenberg model and consistent with the fact that the low-energy scale is controlled by 1D interaction J_d . The calculated curve exhibits a magnetization plateau at the magnetization $M = 1/3$ as expected. The $1/3$ plateau starts from 108 T, which can be accessible by a plus-magnet experiment. Such an experiment is desired to confirm our proposed model. The calculated onset field of the $1/3$ magnetization plateau is 119 T and 130 T for $A = \text{Rb}$ and Cs , respectively (not shown here). The slight increase of the onset field as compared with the $A = \text{K}$ case is attributed to the increase of J_d .

We also examine the dynamical spin structure factor for $\text{K}_3\text{Cu}_3\text{AlO}_2(\text{SO}_4)_4$, defined by

$$S(q, \omega) = -\frac{1}{\pi N} \text{Im} \langle 0 | S_{-q}^z \frac{1}{\omega - \mathcal{H} + E_0 + i\eta} S_q^z | 0 \rangle, \quad (2)$$

where q is the momentum for the triangular unit cell, $|0\rangle$ is the ground state with energy E_0 , η is a broadening

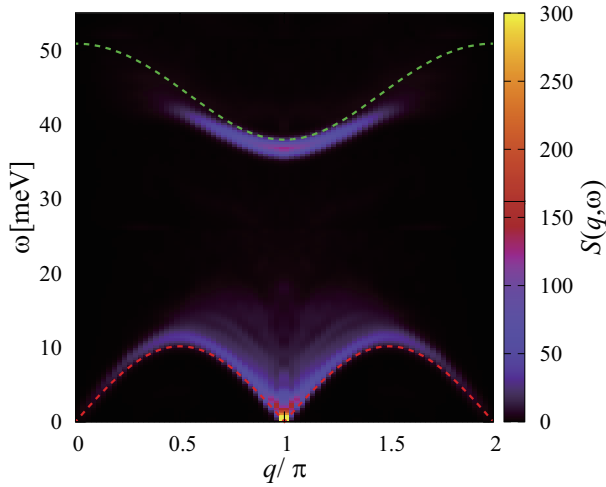


FIG. 4. (Color online) Dynamical spin structure factor $S(q, \omega)$ obtained by dynamical DMRG for a 240-site periodic chain with the exchange interactions for $\text{K}_3\text{Cu}_3\text{AlO}_2(\text{SO}_4)_4$. The red dashed line represents $(\pi/2)J|\sin q|$ with $J = J_d$, while the green dashed line is given by represents $\omega_q = J_5 + J_m \cos q + \frac{1}{4}J_m^2/J_5(3 - \cos 2q)$.

factor, and $S_q^z = N^{-1/2} \sum_i e^{iqR_i} S_i^z$ with R_i being the position of spin i and S_i^z being the z component of \mathbf{S}_i . $S(q, \omega)$ is calculated by using the dynamical DMRG [15] for a $N=240$ -site periodic chain (80 triangular cells). The truncation number $m = 400$ and the truncation error is less than 7×10^{-3} . The value of η is taken to be 0.65 meV.

Figure 4 shows the contour plot of $S(q, \omega)$. At the low-energy region below 10 meV, we find a clear dispersive behavior fitted quite well by $(\pi/2)J|\sin q|$ with $J = J_d$ (the red dashed line). This indicates that the lowest-energy branch comes from the 1D Heisenberg chain connected by the J_d bond. At high energy region around 40 meV, there is a dispersive structure having a minimum at $q = \pi$. This is nothing but the dispersion of a dimer predominantly formed on the J_5 bond. The dispersion relation is well reproduced by the second-order perturbation theory in terms of $J_m (= J'_d)$ giving a dispersion of $\omega_q = J_5 + J_m \cos q + \frac{1}{4}J_m^2/J_5(3 - \cos 2q)$ (the green dashed line) [16, 17], although there is a small deviation. Both the low-energy and high-energy structures should appear in inelastic neutron scattering experiments. In fact, a preliminary experiment for the powder sample of $\text{K}_3\text{Cu}_3\text{AlO}_2(\text{SO}_4)_4$ has shown the corresponding structures [12].

In summary, we have examined the temperature dependence of the magnetic susceptibility for the inequilateral diamond chain compound $\text{A}_3\text{Cu}_3\text{AlO}_2(\text{SO}_4)_4$ ($A = \text{K}, \text{Rb}, \text{and Cs}$) both experimentally and theoretically. The systematic analyses for $A = \text{K}, \text{Rb}, \text{and Cs}$ clearly demonstrate that one of the bonds of the diamond has a strong AFM exchange interaction, producing a dimer. On the other hand, the bond shared by two

triangles in the diamond is FM, in contrast to the azurite where a dimer is formed on this bond. These behaviors accord with the angle-dependence of Cu-O-Cu bond. The dimer controls a high-temperature peak of the magnetic susceptibility as well as a high-energy dispersive structure in the dynamical spin structure factor. On the other hand, a low-energy peak in the magnetic susceptibility and low-energy excitations are controlled by monomers forming a 1D Heisenberg chain. Therefore, the dimer-monomer composite structure is a good starting point of diamond-type quantum spin compounds including azurites, in contrast to the original idea that the diamond chain compounds are highly frustrated. Spin-liquid behaviors observed in the diamond chain compounds are thus attributed to the presence of a 1D Heisenberg chain formed by the monomers. In $\text{A}_3\text{Cu}_3\text{AlO}_2(\text{SO}_4)_4$, the magnetization curve with the 1/3 plateau and inelastic neutron scattering spectra separated by the two energy scales are expected as theoretically demonstrated. Experiments to confirm these predictions are in progress.

This work was supported in part by MEXT as a social and scientific priority issue (Creation of new functional devices and high-performance materials to support next-generation industries GCDMSI) to be tackled by using post-K computer and by MEXT HPCI Strategic Programs for Innovative Research (SPIRE) (hp160222). The numerical calculation was partly carried out at the K Computer, Institute for Solid State Physics, The University of Tokyo, and the Information Technology Center, The University of Tokyo. This work is also supported by Grants-in-Aid for Scientific Research (No. 26287079), Grants-in-Aids for Young Scientists (B) (No. 16K17753) from MEXT, Japan.

* e-mail:katsuhiko.morita@rs.tus.ac.jp

- [1] L. Balents, *Nature* **464**, 199 (2010).
- [2] C. Lacroix, P. Mendels, F. Mila (Eds.), *Introduction to Frustrated Magnetism*, (Springer Series in Solid-State Sciences, 2011), Vol. 164.
- [3] T. Imai and Y. S. Lee, *Phys. Today* **69**, 8, 30 (2016).
- [4] K. Takano, K. Kubo, and H. Sakamoto, *J. Phys.: Condens. Matter* **8**, 6405 (1996).
- [5] K. Okamoto, T. Tonegawa, Y. Takahashi, and M. Kaburagi, *J. Phys.: Condens. Matter* **11**, 10485 (1999).
- [6] K. Okamoto, T. Tonegawa, and M. Kaburagi, *J. Phys.: Condens. Matter* **15**, 5979 (2003).
- [7] H. Kikuchi, Y. Fujii, M. Chiba, S. Mitsudo, T. Idehara, T. Tonegawa, K. Okamoto, T. Sakai, T. Kuwai, and H. Ohta, *Phys. Rev. Lett.* **94**, 227201 (2005).
- [8] H. Jeschke, I. Opahle, H. Kandpal, R. Valenti, H. Das, T. Saha-Dasgupta, O. Janson, H. Rosner, A. Brühl, B. Wolf, M. Lang, J. Richter, S. Hu, X. Wang, R. Peters, T. Pruschke, and A. Honecker, *Phys. Rev. Lett.* **106**, 217201 (2011).
- [9] K. C. Rule, A. U. B. Wolter, S. Süllow, D. A. Tennant, A. Brühl, S. Köhler, B. Wolf, M. Lang, and J. Schreuer,

- Phys. Rev. Lett. **100**, 117202 (2008).
- [10] A. Honecker, S. Hu, R. Peters, and J. Richter, J. Phys.: Condens. Matter **23** 164211 (2011).
 - [11] M. Fujihala, H. Koorikawa, S. Mitsuda, M. Hagihala, H. Morodomi, T. Kawae, A. Matsuo, and K. Kindo, J. Phys. Soc. Jpn. **84**, 073702 (2015).
 - [12] M. Fujihala, H. Koorikawa, and S. Mitsuda, unpublished.
 - [13] Y. Mizuno, T. Tohyama, S. Maekawa, T. Osafune, N. Motoyama, H. Eisaki, and S. Uchida, Phys. Rev. B **57**, 5326 (1998).
 - [14] The Van Vleck paramagnetic susceptibility was estimated using $\chi_{VV} = (N\mu_B^2/\lambda)\Delta g = 9.42 \times 10^{-4}\Delta g$ emu/mol, where N is the number of Cu^{2+} ion, $\Delta g = g - g_e$ is the anisotropy of the gyromagnetic ratio, and $\lambda = 829 \text{ cm}^{-1}$ is the spin-orbit coupling coefficient of Cu^{2+} .
 - [15] S. Sota and T. Tohyama, Phys. Rev. B **82**, 195130 (2010).
 - [16] M. Reigrotzki, H. Tsunetsugu, and T. M. Rice, J. Phys.: Condens. Matter **6** 9235 (1994).
 - [17] O. P. Sushkov and V. N. Kotov, Phys. Rev. Lett. **81**, 1941 (1998).